

## Thermodynamic analysis of solid oxide fuel cell integrated system fuelled by ammonia from struvite precipitation process

Saadabadi, S. A.; Patel, H.; Woudstra, Theo; Aravind, P. V.

### DOI

[10.1002/fuce.201900143](https://doi.org/10.1002/fuce.201900143)

### Publication date

2020

### Document Version

Final published version

### Published in

Fuel Cells

### Citation (APA)

Saadabadi, S. A., Patel, H., Woudstra, T., & Aravind, P. V. (2020). Thermodynamic analysis of solid oxide fuel cell integrated system fuelled by ammonia from struvite precipitation process. *Fuel Cells*, 20(2), 143-157. <https://doi.org/10.1002/fuce.201900143>

### Important note

To cite this publication, please use the final published version (if applicable).  
Please check the document version above.

### Copyright

Other than for strictly personal use, it is not permitted to download, forward or distribute the text or part of it, without the consent of the author(s) and/or copyright holder(s), unless the work is under an open content license such as Creative Commons.

### Takedown policy

Please contact us and provide details if you believe this document breaches copyrights.  
We will remove access to the work immediately and investigate your claim.

# Thermodynamic Analysis of Solid Oxide Fuel Cell Integrated System Fuelled by Ammonia from Struvite Precipitation Process

S.A. Saadabadi<sup>1\*</sup>, H. Patel<sup>1</sup>, T. Woudstra<sup>1</sup>, P. V. Aravind<sup>1</sup>

<sup>1</sup> Process and Energy Department, Faculty of 3mE, Delft University of Technology, Leeghwaterstraat 39, 2628 CB, Delft, The Netherlands

Received July 31, 2019; accepted January 03, 2020; published online ■■■

## Abstract

Energy and exergy performance of ammonia fuelled solid oxide fuel cell (SOFC) integrated system in wastewater treatment plants (WWTPs) is evaluated in this study. Ammonia can be recovered through a struvite precipitation process in the form of an ammonia-water mixture (with 14 mol.% ammonia) and used as a carbon-free fuel. A series of experiments has been conducted for SOFC single cell to evaluate the performance with different ammonia-water mixture ratios. An ammonia-SOFC system was modeled in Cycle Tempo for detailed thermodynamic analysis. The heat from the electrochemical reaction in the SOFC and catalytic combustion in an afterburner is used in the struvite decomposi-

tion process. However, the generated heat is not sufficient to meet the heat demand of the struvite decomposition reactor. To improve the sustainability of the system in terms of heat demand, the system can be integrated into a heat pump assisted distillation tower, meanwhile, the ammonia concentration of the fuel stream increases. Increasing the ammonia concentration to 90 mol.% increases the energy and exergy efficiencies of the SOFC system. The net energy efficiency of the integrated system with a heat pump assisted distillation tower is 39%, based on the LHV of the ammonia-water mixture.

**Keywords:** Ammonia Recovery, SOFC System Modeling, Solid Oxide Fuel Cell, System Integration, Waste to Energy


## 1 Introduction

To decrease the rate of greenhouse gas emissions, the usage of conventional energy resources should be replaced by alternative renewable sources. Recently, energy recovery from wastewater streams has received more attention [1–3]. Raising the quality of discharge water and nutrient removal increases the energy costs of wastewater treatment, which is dominated by the conversion and elimination of nitrogen and phosphorus [4]. Efforts have been made to promote sustainability of the overall sewage treatment and change the wastewater treatment plants (WWTPs) to a net energy producer process [4–8].

Sewage water contains a wide variety of contaminants, such as excess nutrients and organic compounds. Nitrogen is one of the major pollutants in wastewater stream that can cause eutrophication (overly enriched water with minerals and nutrients). Nitrogen in wastewater stream is in the form of organic nitrogen and ammonium. Excessive nitrogen decreases dissolved oxygen levels of the receiving waters and cause toxicity to the aquatic organisms. Hence, the removal of

nitrogen from wastewaters is crucial to reduce harmful effects on the environment [9]. Part of ammonia ( $\text{NH}_3$ ) present in the wastewater can be ionised ( $\text{NH}_4^+$ ) and deionized again (to  $\text{NH}_3$ ). The concentration of ammonia in wastewater can be identified by the total ammonia nitrogen (TAN) value. Based on the pH level and temperature, ammonia toxicity has been reported at concentrations ranging from 0.53 to 22.8 mg L<sup>-1</sup> [10]. Strict regulations for nitrogen discharge from the municipal WWTP leads to significant energy and material costs [9]. There are various techniques like nitrification and denitrification [11–14] to extract nitrogen from the wastewater stream and thereby return it to the atmosphere. Another method is to accumulate nitrogen in the form of ammonia and then remove

[\*] Corresponding author, s.a.saadabadi@tudelft.nl

 This is an open access article under the terms of the Creative Commons Attribution License, which permits use, distribution and reproduction in any medium, provided the original work is properly cited.

it from the wastewater stream. Adding an ammonia removal process in WWTP makes the N-removal process more efficient and economical by reducing the needed areas and volumes of the nitrogen removal step [9].

The accumulated ammonia can be recovered through the struvite precipitation process as this technique certainly possesses some remarkable advantages like reducing the electricity required for nitrogen removal and chemical usages for chemical phosphorus removal [9, 15, 16]. Generally, recovered ammonia from WWTP is used as a fertilizer. However, pure ammonia is considered as a carbon-free fuel. Ammonia can be used as a promising fuel, due to its high hydrogen density, less flammability, and well-known infrastructures associated with transportation and storage (Table 1) [17]. The only drawback of ammonia is its toxicity but can be detected easily due to its strong odour. The concentration of ammonia produced from a precipitation process is as low as 14.3% molar or 13.6% mass fraction (the rest is water vapour). Ammonia-water mixture with such a low concentration of ammonia is not a suitable fuel for conventional energy conversion device like an internal combustion engine. Efficient energy conversion methods such as oxidation of ammonia in the fuel cell can improve energy recovery and reduce the emissions. An energy content comparison and properties of conventional fuels are shown in Table 1.

Fuel cells provide an opportunity to develop thermodynamic systems, which generate electricity on the basis of electrochemical reactions. SOFCs are modular, silent, low-emission and vibration free energy conversion devices. These fuel cells have already been used in different power generation systems, and very high electrical efficiencies (above 60%) have been reported [7]. Even though hydrogen is the most commonly used fuel, SOFC itself can convert chemical energy from a variety of fuels, like hydrocarbon fuels and ammonia [18]. In SOFC application, internal ammonia cracking is observed, due to its high operating temperature (650 °C–900 °C) [19, 20]. Moreover, operating at high-temperature allows using the heat in co-generation or bottoming cycle enhancing the system energy and exergy efficiency [21]. In an integrated ammonia-SOFC system with struvite precipitation process, the generated heat can be used in the decomposition of struvite. To the best of the authors' knowledge, the operation of ammonia fed SOFC with low concentrations of ammonia has not been reported.

An initial objective of this study is to identify the feasibility of integration of the ammonia recovery process (precipitation) from the wastewater treatment plant with SOFC. First, an

overview of energy demand regarding the nitrogen removal in WWTPs is presented, and nitrogen recovery in precipitation process and ammonia production is explained. An experimental study is conducted on a single commercial Ni-GDC (gadolinium doped ceria) electrolyte supported cell with the ammonia-water mixture as fuel. The cell performance is assessed for different ammonia mole fraction at 800 °C. Subsequently, system modeling is carried out to evaluate the ammonia-SOFC system efficiency in such a way that the ammonia-water mixture (with low ammonia concentration) is used as fuel, and the generated heat is applied in the ammonia recovery process. Then, this system is optimized to improve the system efficiency by increasing the ammonia concentration before feeding to SOFC and evaluate the performance of the developed model thermodynamically.

## 1.1 Ammonia Production

The main industrial procedure for ammonia production is the Haber–Bosch process. Ammonia is produced through the reaction of  $H_2$  and  $N_2$  under high temperatures and pressures. The energy demand (mostly electricity) of this process is around 28 MJ  $kg^{-1}$   $NH_3$  (0.48 MJ  $mol^{-1}$   $NH_3$ ) [22, 23] which is higher than the low heating value (LHV) of ammonia (see Table 1), and releases 1.92–3.82 kg  $CO_2$   $kg^{-1}$   $NH_3$  [24, 25]. However, ammonia can be produced from nitrogen-rich sources through some minimal carbon footprint techniques. For instance, several biological and physicochemical treatment techniques have been considered and developed to remove nitrogen from wastewater streams [26].

## 1.2 Nitrogen Removal in WWTPs

### 1.2.1 Conventional Techniques

Conventional biological treatment like aerobic digestion is using most typically nitrogen removal processes in wastewater treatment plants, due to lower capital costs and fewer operational problems [27]. However, the operating costs are high, due to the high amount of dissolved oxygen (DO) demand, which is the essential parameter in the aerobic digestion process. The DO concentrations generally range between 0.5 to 2.0 mg  $L^{-1}$   $_{water}$  based on the type of influent and aeration conditions [11, 28] and makes total aeration energy demands very high. The energy requirement for wastewater treatment based on the treatment method can reach to 15.2 MJ  $m^{-3}$  and 53% of that is attributed to aeration [29].

In the 18th and 19th century, several processes were investigated to treat the digester liquid with nitrification/denitrification by the addition of organic carbon sources. These processes are based on the biological transformation of ammonia to nitrate. Denitrification occurs during the anoxic period, and nitrification takes

Table 1 Ammonia in comparison with other conventional fuels (in liquid phase).

Fuel	Density / $kg\ L^{-1}$	LHV / $MJ\ kg^{-1}$	LHV / $MJ\ L^{-1}$	$H_2$ density / $kg\ H_2\ L^{-1}$
Hydrogen	0.07	120.1	8.4	0.070
Ammonia	0.76	18.6	14.1	0.136
Methane	0.47	50.1	23.3	0.116
Gasoline	0.70	42.5	29.8	0.110

place during the aerobic period. Through the biological nitrogen removal, first organic nitrogen converts to ammonium ( $\text{NH}_4^+$ ). Then, ammonium reacts with oxygen to produce nitrite ( $\text{NO}_2^-$ ), which is followed by oxidizing of nitrite to nitrate ( $\text{NO}_3^-$ ) during the nitrification process. Finally, produced nitrate converts to nitrogen by heterotrophic bacteria through the nitrification process in the presence of an external carbon source determined by biochemical oxygen demand (BOD). Oxygen demand for complete nitrification of ammonium is  $4.57 \text{ g O}_2 \text{ g}^{-1} \text{ N}$  [13]. Additionally, some amount of alkalinity is required for nitrification reactions. It is also claimed that  $4 \text{ mg L}^{-1}$  of DO is sufficient to achieve sustainable nitrification. Electricity demand for the nitrification (aeration) is  $17 \text{ MJ kg}^{-1} \text{ N}$  [30], which can be about 70–80% of the total energy demand of a municipal WWTP [31].

In the late 90s, anaerobic ammonium oxidation (anammox) process was introduced. Strous et al. [32] claim that this process can significantly reduce aeration energy demands and requires no organic carbon source. However, nitrogen removal through an advanced Sharon/Anammox process still requires a considerable amount of power ( $14 \text{ MJ kg}^{-1} \text{ N}$ ) [16]. Even with applying new nitrogen removal techniques such as using anaerobic membrane bioreactors, electrical energy required is still high, and energy requirement of around  $18.3 \text{ MJ kg}^{-1} \text{ N}$  (considering a TAN of  $100 \text{ mg L}^{-1}$ ) is reported in literature [33]. On the other hand, there is an alternative approach to convert nitrogen to ammonia in order to use it for different applications.

A conventional wastewater treatment plant is shown in Figure 1. The concentration of organic compounds and nutrients in the wastewater stream is increased through primary and secondary sewage treatment. The activated sludge stream is more suitable for use in the waste-to-energy strategy [7]. Activated sludge is conveyed to the anaerobic digester, where biogas is produced from organic materials. The concentration of ammonia/ammonium is high in the influent stream to anaerobic digestion (AD). Moreover, ammonia concentration also increases during the AD process. Ammonia removal is essential, because high ammonia concentration ( $4\text{--}5 \text{ g NH}_3\text{-N L}^{-1}$ ) is an

inhibitor of methanogenic bacteria [34,35]. The level of toxicity depends on AD conditions such as temperature, pH, retention time and concentration of organic and inorganic compounds inside the anaerobic digester [36]. Furthermore, removing ammonia from AD also decrease the DO demand in aeration due to the low concentration of ammonia in the recirculated water stream [16]. This reduces the energy demand during the aeration process.

Several studies have been carried out on nitrogen removal/recovery processes like direct stripping either with air or with biogas [37,38], ion exchange [39], electrodeionization [40], pre-treatment by microwave radiation [41], electrodialysis and pre-evaporation (hydrophobic) for a wide range of total nitrogen (TN) concentration and different wastewater resources [42–44]. For instance, the energy demand for ammonia removal through the air stripping process is around  $40\text{--}50 \text{ MJ kg}^{-1} \text{ N}$  [16]. Luther et al. [45] have investigated ammonia recovery from human urine (with a high concentration of ammonium) by an electrochemical cell. The electrical power demands for different concentration of ammonium are shown in Table 2. It should be noted that during this process, some amount of hydrogen is produced, which is worth approximately  $15.5 \text{ MJ kg}^{-1} \text{ N}$  and decreases the overall energy demand for ammonia recovery. This study is focused on the chemical precipitation process for ammonia recovery with heat generated from an SOFC stack.

### 1.2.2 Precipitation Process

Generally, the Ammonia-Nitrogen ( $\text{NH}_3\text{-N}$ ) and Ammonium-Nitrogen ( $\text{NH}_4^+\text{-N}$ ) concentration are moderately low in

Table 2 Ammonia extraction from synthetic and undiluted human urine using an electrochemical cell.

Ammonium concentration flux / $\text{gN m}^{-2} \text{ d}$	Current efficiency / %	Electrical power demand / $\text{MJ kg}^{-1} \text{ N}$
$384 \pm 8$	$61 \pm 1$	43
$275 \pm 5$	$55 \pm 1$	47

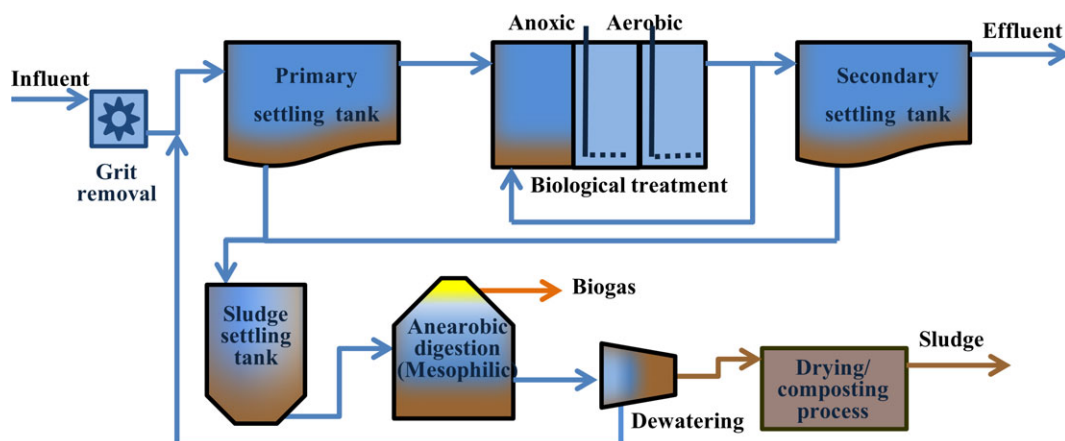
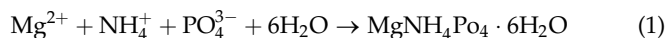
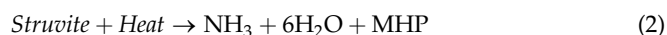


Fig. 1 Conventional wastewater treatment plants, including nitrogen removal process (aeration) and anaerobic digestion.

the wastewater stream (roughly  $50 \text{ mg L}^{-1}$ ) [46]. But, the concentration is higher after primary wastewater treatment. Struvite precipitation is one of the interesting methods for ammonia recovery when the concentration of ammonium is in the range of  $0.1$  to  $5 \text{ g N L}^{-1}$  [47]. Magnesium ammonium phosphate (MAP), so-called struvite, is crystallized by adding magnesium ion to wastewater in order to gradually increase the pH level (Eq. (1)). To achieve high-purity struvite, it is recommended to raise the pH value to  $9.0$ – $9.5$  [48, 49]. Struvite crystals are formed inside the reactor with an average size of  $42$  to  $80 \text{ }\mu\text{m}$  [16].



Next, in the decomposition reactor, the struvite crystals can be decomposed into magnesium hydrogen phosphate (MHP) and ammonia Eq. (2) by absorbing heat. MHP is recycled to the struvite reactor to remove ammonium from the wastewater. Indeed, the residues of struvite decomposed could be used as P and Mg sources, reducing operation costs of struvite precipitation process. In addition, part of the MHP can be used in the phosphate processing industry, as an environmentally friendly alternative to mined phosphate ore or as a fertilizer. Struvite is thermodynamically unstable, and dehydration starts just above room temperature [50]. Sarkar [51] found that the maximum decomposition takes place at  $106^\circ\text{C}$  based on the results from derivative thermogravimetric analysis (DTGA). The remained MHP is returned to the crystallization reactor to react with ammonium from the wastewater stream again (Figure 2).



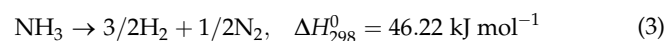
This method is known as a cost-effective technique in comparison to aeration of elemental nitrogen gas in conventional WWTPs [16]. Energy demands of struvite production are estimated around  $9.3 \text{ MJ kg}^{-1} \text{ N}$  electricity ( $5.6 \text{ MJ kg}^{-1} \text{ N}$  for the process itself). Other energies, including the energy need for production of magnesium and phosphorus at the beginning of the process, is not considered [30].

Theoretically, the stream released from the pyrolysis of struvite contains an ammonia-water mixture with  $14.3 \text{ mol.}\%$  ( $13.6 \text{ mass}\%$ ) ratio of ammonia. The decomposition stage of the struvite needs around  $2,650 \text{ kJ kg}^{-1}$  of the produced stream (see Appendix). Moreover, phosphorus reduction is also

another advantage of this method and phosphate can be recovered from struvite decomposition. Phosphate is a limited source in the environment and essential material in the food industry, which is also used as a fertilizer. Scheme of ammonia production from wastewater influent is shown in Figure 2.

### 1.3 Ammonia-fuelled SOFC

Ammonia recovered as a hydrogen carrier fuel can be cracked to hydrogen at high temperature. Ammonia cracking reaction is endothermic and starts at  $405^\circ\text{C}$  Eq. (3) and complete conversion of the ammonia takes place at  $590^\circ\text{C}$  [52]. The normal operating temperature of SOFC is in the range of  $650$  to  $850^\circ\text{C}$ . So, ammonia cracking can take place inside the SOFC.



A lot of studies have been carried out on the thermal decomposition of ammonia with different catalysts [53]. Chellappa et al. [54] have investigated the kinetics of pure ammonia cracking over a Ni-Pt/ $\text{Al}_2\text{O}_3$  catalyst at a diverse range of temperatures. The reaction rate was first order with respect to ammonia partial pressure at the temperature between  $524$  and  $690^\circ\text{C}$ .

$$r = k_0 \exp\left(-\frac{E_a}{R \cdot T}\right) P_{\text{NH}_3} \quad (4)$$

The activation energy ( $E_a$ ) of ammonia cracking is found to be about  $196.2 \text{ kJ mol}^{-1}$ . The coefficient  $k_0$  has been determined as  $4.0 \times 10^{15}$  for Eq. (4) [53]. Conducted experiments on different kind of electrolytes and anode materials of SOFCs indicate that Ni-based anode is a proper catalytic material for ammonia cracking and more than  $90\%$  ammonia cracking can be achieved for ammonia-SOFC at a high temperature around  $800^\circ\text{C}$  [19, 55, 56]. An ammonia cracking of  $99.996\%$  has been reported for a Ni-YSZ (Yttria-stabilized zirconia) anode at  $800^\circ\text{C}$ , which is close to the equilibrium composition [57]. Many studies have been conducted to assess the direct ammonia-fuelled SOFCs potential [19, 53, 57, 58]. Experimental studies illustrate that the performance of the SOFC running on pure ammonia is close to hydrogen-fuelled one [59–61]. Comparable cell performances are reported on pure ammonia in comparison to humidified hydrogen when operated at a higher temperature (roughly around  $800^\circ\text{C}$ ) [20, 57, 62, 63]. Furthermore, a better SOFC system performance is reported due to less cooling required for ammonia-SOFC stacks [57].

Additionally, by using ammonia as an alternative fuel for SOFC,  $\text{NO}_x$  formation can be prevented, because of the low-temperature reaction in comparison with typical combustion devices [64]. Generally, in ammonia-

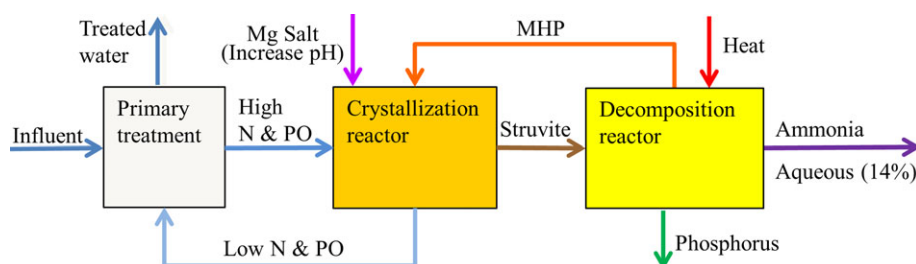


Fig. 2 Scheme of struvite precipitation process.

fed SOFC studies, it was assumed that the partial oxidation reaction forming NO is energetically less favorable. Later, investigations show that the  $\text{NO}_x$  concentrations in the SOFC off-gas are negligible [61, 65].

Ammonia-SOFC modeling studies have been conducted for different operating conditions. Farhad and Hamdullahpur [66] proposed a conceptual design of a portable ammonia-fuelled SOFC system. The results predicted through the simulation system confirm that the first-law efficiency of 41.1% is achievable with the system operating at a cell voltage of 0.73 V and fuel utilization of 80%. Rokni [67] has developed a hybrid system for different types of fuel, like ammonia by a general energy system simulation tool. The obtained system efficiency for the pure ammonia fuelled SOFC was around 58%, the lowest value among different types of fuel. However, it is found that energy efficiency is not decreasing by lowering the SOFC operating temperature. Baniasadi and Dincer [68] have studied an ammonia-SOFC system with SOFC- $\text{H}^+$  technology for vehicular applications. They have focused on energy and exergy analyze of this system by varying fuel utilization and current density. An energy efficiency of 42% is achieved in this system operating at 700 °C fuelled with pure ammonia at a current density of 1,400 A m<sup>-2</sup> and fuel utilization of 80%. Patel et al. [21] have found total exergy efficiency of 69.8% for a high-temperature SOFC-GT system fed with pure ammonia at a cell voltage of 0.78 V and cell resistance of  $5.0 \times 10^{-5} \Omega \text{ m}^2$  (at 950 °C). Results show that 55.1% of the exergy is converted to electrical power in the SOFC stack.

## 2 Experimental

So far, many studies only focused on using high concentrations of ammonia or hydrogen ammonia-mixture for SOFC [21, 66, 69], however, as mentioned, the concentration of ammonia from the struvite decomposition reactor is as low as 14 mol.% (based on the stoichiometric ratio) and the rest is water vapour. If the ammonia concentration in the fuel mixture decreases, the hydrogen concentration of ammonia cracking decreases as well. This leads to a low hydrogen partial pressure in fuel gas flow, which reduces the cell reversible potential. The performance of ammonia-SOFC with low concentration has not been comprehensively studied.

### 2.1 Experimental Approach

A series of experiments have been conducted to evaluate the performance of SOFC with different ammo-

nia-water mixtures at 800 °C. The schematic of the setup used is shown in Figure 3. A commercial Ni/GDC electrolyte-supported cell (ESC) with an activated area of 81 cm<sup>2</sup> is used in this experiment. Inlet gas composition is supplied from gas bottles, and the flow rate and the ratio of the ammonia-water mixture are adjusted by using mass flow controllers (MFC) and the controlled evaporation and mixing (CEM) system. The anode inlet gas is preheated (trace heating) to prevent steam condensation inside the pipe. For the cathode side, the air is simulated by mixing 1,200 N mL min<sup>-1</sup> nitrogen and 320 N mL min<sup>-1</sup> oxygen. The current-voltage (*I*-*V*) characterization is performed in the potentiostatic control mode by an electronic impedance spectroscopy (EIS) device (Gammy FC-350). The outlet gas (dry based) composition can be analyzed by a micro gas chromatography (GC) device (Agilent 490). The outlet gas can be sampled at the outlet of the fuel cell ceramic block, and the concentration of ammonia can be measured by a Dräger sampling tube. The cell temperature is measured with a k-type thermocouple placed very close to the anode side.

### 2.2 Experimental Results

#### 2.2.1 Ammonia Cracking

After the cell reduction process with the hydrogen-nitrogen mixture, a mixture of ammonia (200 N mL min<sup>-1</sup>) and nitrogen (600 N mL min<sup>-1</sup> as carrier gas) is used to check the feasibility of ammonia cracking inside the fuel cell block (cell holder) itself. The outlet gas from the anode channel is analyzed by micro GC. The same test is conducted with an equivalent amount of hydrogen and nitrogen (300 and 700 N mL min<sup>-1</sup>  $\text{H}_2$  and  $\text{N}_2$ , respectively). The results of the micro GC show

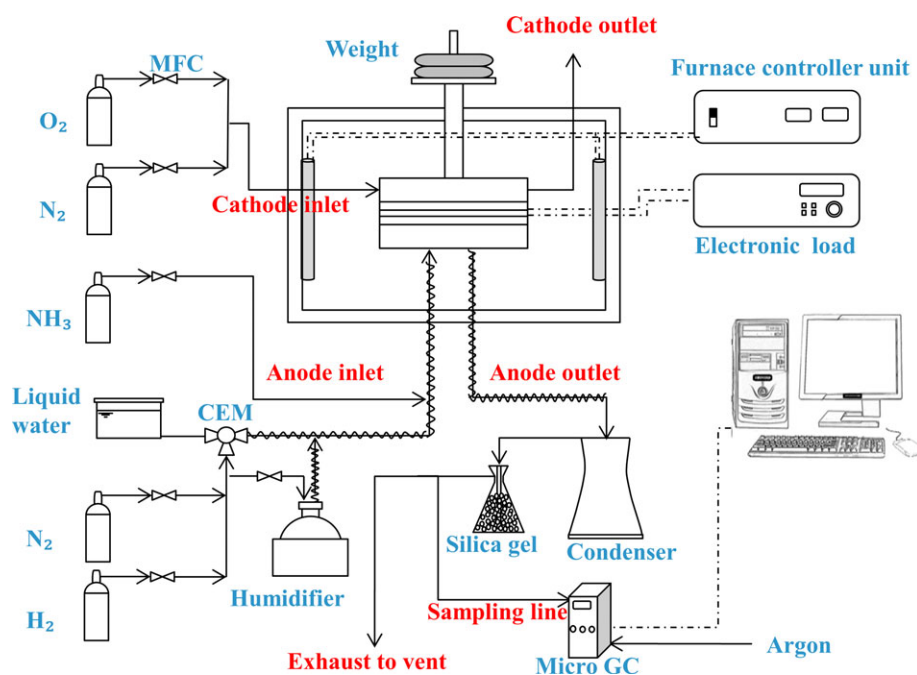


Fig. 3 Scheme of the experimental test station.

that the  $H_2/N_2$  ratio of the outlet gas for both ammonia and hydrogen fuelled SOFC are 0.39. This implies that ammonia is cracked into nitrogen and hydrogen at  $800^\circ\text{C}$  in this setup. The concentration of ammonia at the outlet is also measured by a Dräger sampling tube, and it was less than 1,000 ppm, which gives an ammonia cracking of 99.6%.

## 2.2.2 Ammonia in Comparison to Hydrogen

Subsequently, pure ammonia is used as a fuel ( $350\text{ N mL min}^{-1}$ ). The polarization curve of this test is shown in Figure 4. Then, an equivalent amount of hydrogen and nitrogen ( $525$  and  $175\text{ N mL min}^{-1}$   $H_2$  and  $N_2$ , respectively) is fed to SOFC. The performance of the cell with ammonia fuel is comparable with hydrogen/nitrogen mixture fuel. For both tests, the oven temperature was constant but, the cell temperature is slightly lower (around  $7^\circ\text{C}$ ) with ammonia fuel, due to the endothermic reaction of ammonia cracking, which causes higher cell ohmic resistance for Ammonia-fed SOFC. This is in agreement with results reported by Cinti et al. [56].

## 2.2.3 Ammonia-water Mixture

Various ammonia-water mixtures are used to evaluate the influence of steam concentration on cell performance. The total flow rate and ammonia flow (for the anode) are  $1,000\text{ N mL min}^{-1}$  and  $200\text{ N mL min}^{-1}$ , respectively. A fuel utilization of 56% achieved in the test with pure ammonia at a current density of  $3,000\text{ A m}^{-2}$ . The oven temperature was constant for all gas compositions. The polarization ( $I$ - $V$ ) curves of these gas compositions are shown in Figure 5. Low concentration of steam (15%) is provided by a humidifier, and higher steam concentrations are supplied by a controlled evaporation and mixing (CEM) system. The nitrogen gas stream is required to carry steam before mixing with the pure ammonia stream. Results show the possibility of operating SOFC with a high concentration of steam at  $0.7\text{ V}$  and  $800^\circ\text{C}$ . These are the conditions that will be used in the system modeling section of this study. Increasing ammonia concentration increases obtained current density. The area specific resistance (ASR) is in the order of  $1.1 \times 10^{-4}\ \Omega\text{ m}^2$ .

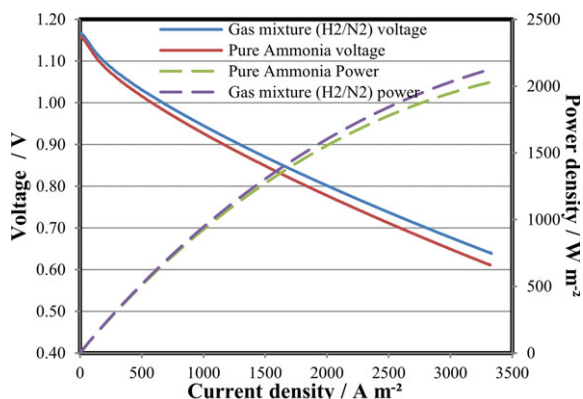


Fig. 4 Polarization ( $I$ - $V$ ) curves for an SOFC fuelled with pure ammonia and hydrogen/nitrogen mixture at  $800^\circ\text{C}$ .

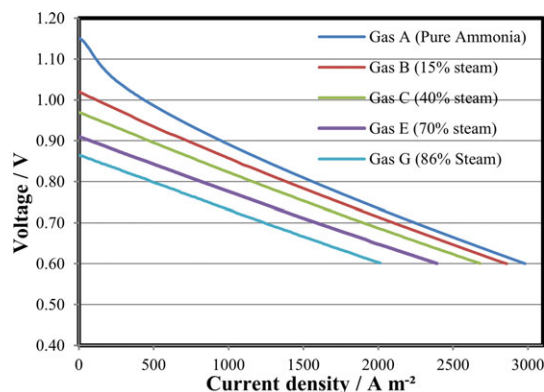


Fig. 5 Polarization ( $I$ - $V$ ) curves for an SOFC fuelled ammonia-water mixture with different ammonia concentration.

## 3 System Modeling Study

### 3.1 Thermodynamic Analysis and Modeling Approach

Exergy analysis can be employed to improve the energy efficiency of systems, by minimizing of irreversibilities. For instance, electrochemical oxidation is more reversible in comparison with the combustion process. System optimization can also be carried out by improving system configuration in order to decrease the irreversibilities. Based on works reported in literature, there are some studies on SOFC system modeling with different system configurations and types of fuels [21, 69, 70]. A Cycle-Tempo model has been developed by H. Patel et al. [21] to evaluate an SOFC-gas turbine system with different fuels, including pure ammonia. It is claimed that the energy efficiency of ammonia fed SOFC is higher than hydrogen, but the exergy efficiency is slightly lower. The highest exergy destruction is attributed to the fuel cell itself and exergy losses in the stack (exhaust) is almost the same for all types of fuels.

This study analyzes the energy and exergy efficiency of an integrated power generation system based on an ammonia fed SOFC in which ammonia is produced through the decomposition of struvite. The influence of individual components on the overall system efficiency is evaluated by the exergy analysis. The system performance is improved by the optimization of operating conditions. It is aimed to convert an energy consuming process step (nitrogen removal in WWTP) to an energy-producing process step.

### 3.2 System Description

After the primary wastewater treatment process, effluent with a high concentration of nitrogen is conveyed to the crystallization reactor. Struvite is extracted from the sludge stream in this reactor and carried to the decomposition reactor. Ground struvite is heated up in this reactor where the ammonia-water mixture is evaporated, and the MHP is sent back to the crystallization reactor. Ammonia water mixture can be condensed and stored in a vessel, or the vapour can be con-

veyed directly to the SOFC as a fuel. Potential contaminants and particles in the ammonia-water vapour stream can be removed by using a filter before entering the SOFC stack. Since the fuel utilization is set in the range of 80%, an afterburner is used to burn the remaining hydrogen gas in anode exhaust. The heat generated from the electrochemical reaction of fuel in SOFC and burning hydrogen in the afterburner can be used for the struvite decomposition process. The flow diagram (Figure 6) shows a simplified integrated system of the ammonia precipitation process with ammonia fuelled SOFC. The operating temperature would be between 700 °C to 850 °C, because at a higher temperature (up to 950 °C) trace of  $\text{NO}_x$  (0.5 ppm) has been observed [71].

### 3.3 Model Description

Cycle-Tempo is a software developed at Delft University of Technology to thermodynamically evaluate power cycles (including fuel cell systems). Equilibrium calculations are employed to calculate the fluid properties and energy production/consumption in each apparatus. Calculation methods employed and detailed information pertaining this is explained in detail in the manual of this software [72]. Mass and energy balance equations are used to calculate mass flow in each apparatus. The airflow for the cathode side is calculated based on the cooling requirement of the SOFC stack. It should be mentioned that the system efficiency is calculated based on absorbed energy, the LHV of the ammonia-water-mixture. The filter (after the decomposition reactor) is not included in the system modeling, as it has no influence on the thermodynamics of the system. Some of the major input parameters used in the model are illustrated in Table 3.

This Ammonia-SOFC integrated system is operating at atmospheric pressure. The cell resistance is set  $1.0 \times 10^{-4} \Omega \text{ m}^{-2}$  at a cell temperature of 800 °C. This is in agreement with the cell resistance reported in literature at this operating temperature and also measured in Section 3 of this study [71]. Aqueous ammonia with 13 mass % ammonia (14 mol.%) in water

Table 3 Input parameters for ammonia-SOFC system model in Cycle Tempo.

Parameter		Value
Cell operating temperature		750–800 °C
Cell operating voltage		0.6–0.75 / V
Fuel utilization (per-pass utilization)		76–80%
Cell resistance		$1.0 \times 10^{-4} / \Omega \text{ m}^{-2}$
Current density		1,400–2,200 / A m <sup>−2</sup>
SOFC temperatures:	Inlet	650–680 °C
	Outlet	775 °C
	Operating (reaction)	800 °C
Compressor:	Isentropic efficiency	75%
	Mechanical efficiency	98%
Pressure drops:	Fuel cell	0.005 / bar
	Heat exchanger	0.025 / bar

with a flow rate of  $10 \text{ kg s}^{-1}$  is assumed as SOFC fuel. First, ammonia and air flows are preheated in heat exchangers (Figure 7) and then mixed with the anode and cathode gas recirculation flows, respectively. The overall fuel utilization (based on fresh fuel in pipe #101) is fixed. However, the per pass fuel utilization (based on fuel used in the SOFC stack) can change based on the anode and cathode gas recirculation ratios. These ratios are determined based on the outlet temperatures of the fuel and air in the heat exchanger #405 and #403, respectively. Increasing the temperature of the fuel in pipe #104 decreases the gas recirculation ratio for the anode side and results in increasing the per pass fuel utilization. The temperature of fuel at the inlet of the SOFC stack reaches to 675 °C. The temperature for air (cathode side) is set to 650 °C. The fuel cell exhaust still includes some hydrogen gas ( $U_f = 80\%$ ) which can be burnt in a catalytic afterburner (apparatus 301). Then, the flue gas is passed through heat exchangers to preheat inlet streams, air flow for the cathode side and ammonia-steam mixture flow for the anode side. This leads to

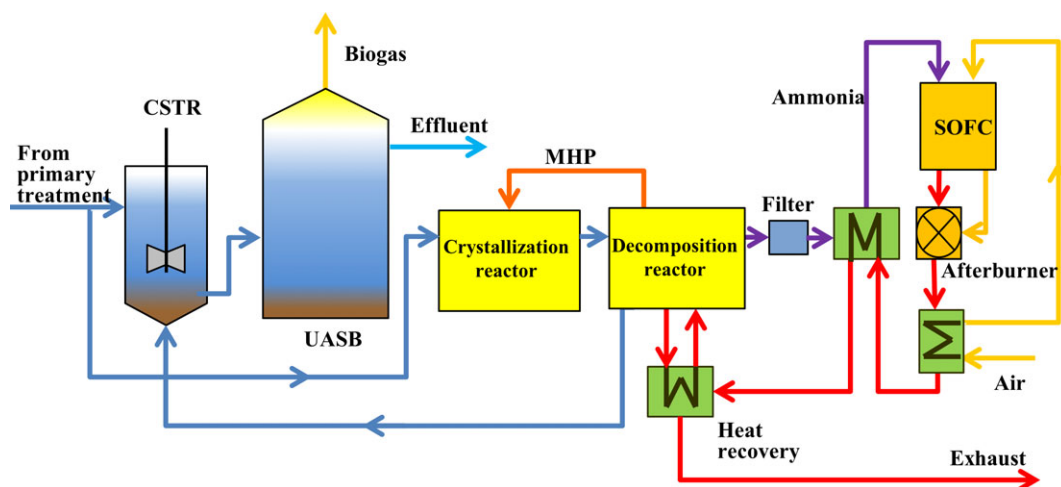


Fig. 6 A Simplified layout for implementation of ammonia precipitation process in WWTPs with SOFC.

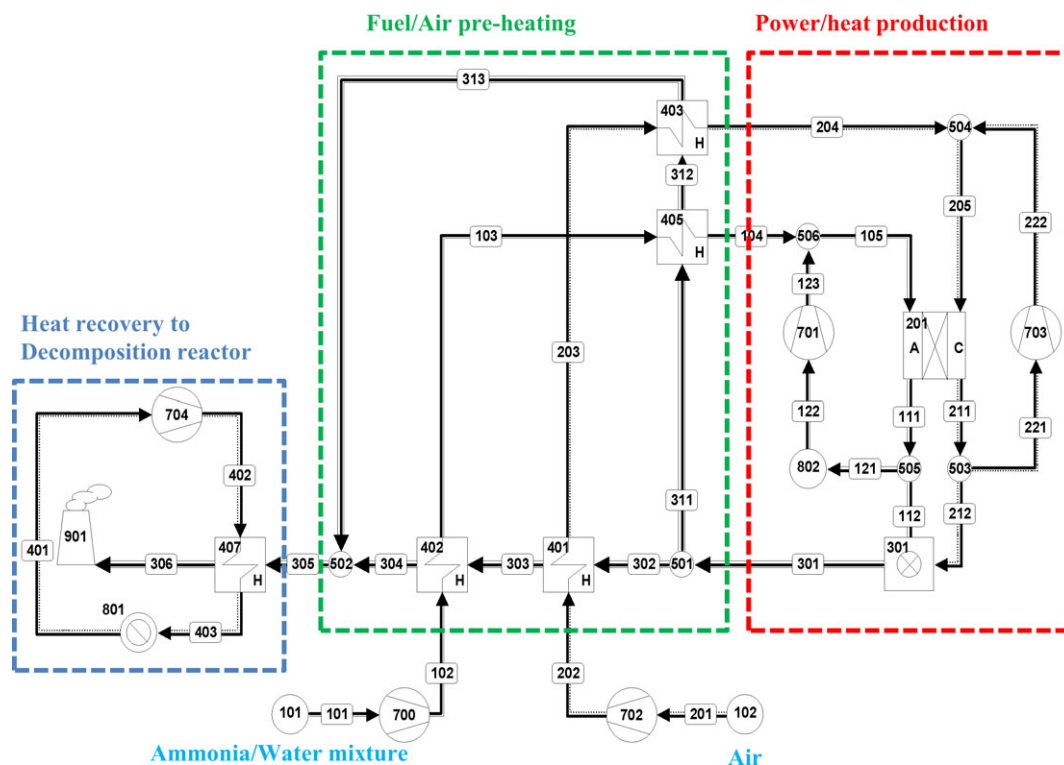


Fig. 7 Simplified Ammonia-SOFC system model in Cycle-Tempo with ammonia decomposition reactor.

better heat recovery and a decrease in thermal stress inside the SOFC. Ammonia cracking takes place inside the fuel cell. All heat exchangers are assumed to be in counter-flow configuration. There is still residual heat, which can be used in the struvite decomposition process (see Appendix). A heat sink is considered to simulate the decomposition reactor in the struvite precipitation process. Air circulation is used to transfer heat from flue gas to the decomposition reactor. It appeared that the outlet flue gas temperature of the heat exchanger (407) is high enough to avoid condensation of water-vapour in this heat exchanger.

## 4 Modeling Results and Discussions

### 4.1 Operating with Low Ammonia Concentration

As a first step, ammonia water mixture with an ammonia concentration of 14 mol.% is used as a fuel for this model. The experimental results show the feasibility of using low concentration ammonia as a fuel for operating an SOFC. Results from computations showed that the fuel cell produces 12.42 MW electrical power at 0.66 V cell voltage and a current density of  $1,500 \text{ A m}^{-2}$ , which is in line with experimental results (Figure 5). The overall fuel utilization (based on fresh fuel injected into the system) is set at 83%, while the per-pass utilization obtained is less than 79.1%.

In this system, the fuel and air exhausts from the SOFC stack are partially recirculated to the stack and mixed with preheated fuel and air, respectively. The recycle ratio is the ratio of recirculated flow back to the SOFC from the outlet

flow. The fuel and air recirculation ratios are 0.12 and 0.66, respectively. The oxygen utilization (per-pass) is roughly 50%. The air recirculation reduces the oxygen-utilisation per-pass. The electrical energy requirements for compressors are 6 and 32.3 kW for anode gas and air recirculation, respectively. Ammonia gas completely cracks inside the SOFC stack, and there is still hydrogen in the anode off-gas stream. Hydrogen combustion takes place in the afterburner with low air-fuel ratios ( $\lambda = 1.5$ ). With this system configuration, the net energy efficiency achieved is 48.5%, and the exergy efficiency is 39%. Operating the ammonia-SOFC system in these conditions provides 12.35 MW heat for struvite decomposition reactor, which is not sufficient for producing  $10 \text{ kg s}^{-1}$  of ammonia-water fuel. The remaining heat demand for struvite decomposition (14.15 MW) can be supplied from biogas combustion produced in an anaerobic digestion reactor [7]. This brings the overall efficiency (including struvite decomposition) to 31.8% (based on ammonia and biogas LHV values).

Energy/exergy losses in this system are attributed to the irreversibilities in heat exchangers, mixing nodes, fuel cell and afterburner (combustor). Most exergy loss takes place in the fuel cell, heat exchangers, especially in apparatus 401, 402, and 407 due to high temperature-differences between the flows. The exergy efficiency of SOFC stack ( $W/(Ex_{in}-Ex_{out})$ ) in this system is 81%, while 9.2% of total exergy destruction occurs in the fuel cell stack (Figure 8). High concentration of nitrogen and steam in the fuel stream cause dilution of fuel, which results in reducing the air requirement (for SOFC stack cooling) in the cathode side. Additionally, the endothermic reaction of ammonia cracking further decreases the air

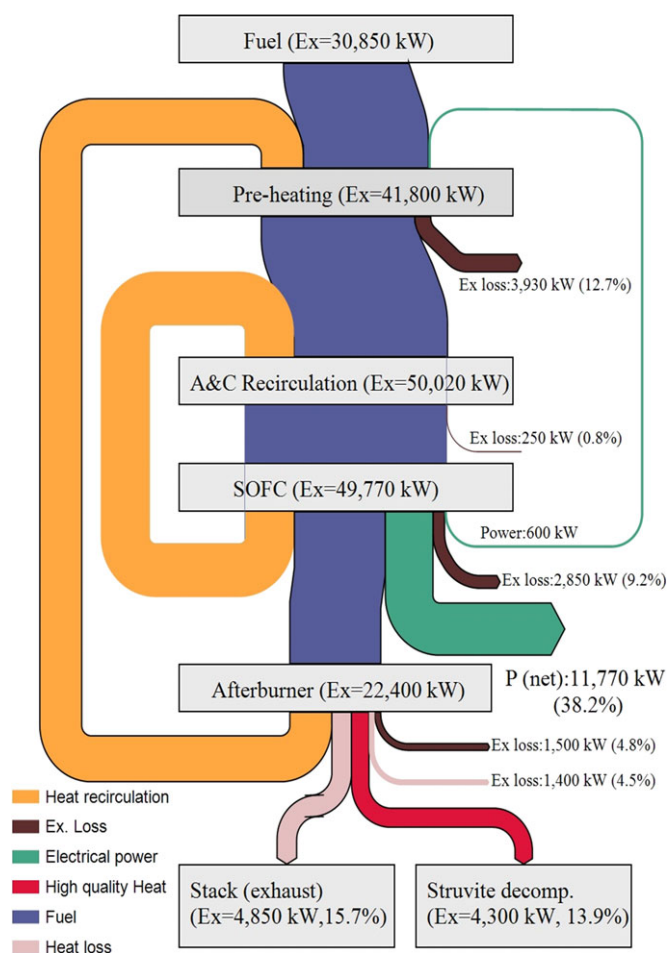


Fig. 8 Distribution of exergy losses in Ammonia-SOFC model with ammonia concentration of 14 mol.%.

requirement. Decreasing air requirements increases the exergy efficiency of the system. The heat from out flow (to the exhaust stack) can still be used for other processes since the temperature is around 90 °C. For instance, it can be used in the thermal pre-treatment of sludge for anaerobic digestion. Exergy destruction of the ammonia-SOFC system is shown in Figure 8. The high amount of exergy loss (15.7%) to the stack (the exhaust, apparatus #901) should be decreased to make this system more efficient. Part of the exergy flow (4.3 MW out of 12.35 MW<sub>th</sub>) is delivered to the struvite decomposition reactor for the precipitation process. In spite of low ammonia concentration, the energy and exergy efficiencies of this system are comparable with results reported in literature [66, 68].

## 4.2 Increasing Ammonia Concentration

Regarding the ammonia production process from struvite, the ammonia concentration would be 14.3 mol.% (based on the stoichiometric ratio shown by Eq. (2)). In the previous section, the ammonia-SOFC system efficiency has been evaluated with respect to the struvite decomposition process. There is a possibility to increase the ammonia concentration in the inlet stream by applying the distillation method. Thus, it is interesting to investigate whether increasing ammonia concentration improves net system efficiency.

### 4.2.1 Distillation Process

Distillation is a physical separation process that used to remove components from a liquid phase by selective boiling and condensation. The liquid stream is being brought in contact with a gas stream in each stage (tray) inside a distillation tower [73]. A distillation tower can be used to supply an ammonia-water mixture, rich in ammonia, to be fed to the SOFC. The process was found to be effective while the nitrogen discharge regulations (concerning the ammonia left in the waste-water) are met.

Separation of the most volatile components (in this case NH<sub>3</sub>) from the liquid phase (water), can be accomplished by using multiple stages in series with a reflux ratio between stages [73]. However, in practice, specifically for ammonia-water mixture, there are limits to the number of stages and the reflux ratio in this process [73]. First, the ammonia-water mixture (in vapour phase) is fed into the bottom stage of the distillation tower. Because of the high temperature, the vapour mixture rises through the packed column, and this mixture is condensed following to the top of the tower. A larger ammonia concentration is achieved after condensation of water vapour in the distillation tower. Then, based on the reflux ratio, part of the condensed mixture flows back into the distillation tower, and flow with high ammonia concentration is discharged. Typically a reboiler is used to provide heat to the bottom of distillation towers, however, in this case, because of the high temperature of the flow from the struvite decomposition reactor (106 °C), the presence of a reboiler is not required for the distillation tower in this system. For more information and details regarding the distillation tower, see [73–75].

A simplified ammonia recovery model (based on distillation) has been developed using Aspen plus software to determine energy consumption through the distillation process. Various reflux ratios have been applied to increase the ammonia concentration (Table 4).

Table 4 Ammonia recovery results from Aspen plus distillation tower model (without reboiler equipment) at atmospheric pressure.

Influent temperature / °C	Reflux ratio	Number of trays	Top stream (vapour)			Condenser heat duty / MW	Bottom stream (liquid)	
			Ammonia mol. %	Temperature / °C	Flow rate / kg s <sup>-1</sup>		flow rate / kg s <sup>-1</sup>	Ammonia / ppm
106	5.3	5	90	50	1.46	-19.7	8.54	2,340
106	3.4	5	60	76	2.18	-18.0	7.82	1,923
106	1.3	4	30	90	4.32	-13.1	5.68	1,763

The vapour stream in a distillation tower should be cooled down further to achieve higher ammonia concentrations. For instance, an ammonia concentration of 90% can be obtained by decreasing the vapour stream temperature to 50 °C. Heat duties of the condenser for different reflux ratios are illustrated in Table 4. Low-temperature water is used to fulfil the cooling in the condenser of the distillation tower. A heat pump is used to decrease the temperature of circulating water. In the next section, integration of the struvite decomposition reactor, heat pump and distillation tower are explained.

As explained in the previous section, the vapour stream of the distillation tower needs to be cooled down in the condenser of distillation tower (#1 Figure 9). For instance, with a reflux ratio of 5.3, the condenser heat duty is 19.7 MW at the

In order to simulate the heat pump assisted distillation tower, a Cycle-Tempo model is developed (Figure 10). A water cycle is required to transfer heat from the condenser of the distillation tower to the evaporator of the heat pump. Then, heat is transferred to the decomposition reactor by this heat pump, whereas pure ammonia is used as a refrigerant [77]. The condenser of the distillation tower is modeled as a heat source (apparatus 301 in Figure 10). The model calculates all flow rates required for heat transmission. For instance, the water flow rate is  $195 \text{ kg s}^{-1}$  in pipe 301. In heat exchanger 103,  $100 \text{ kg s}^{-1}$  of wastewater is heated up to  $35^\circ\text{C}$ , which transfers around 8.4 MW heat. In the evaporator (heat exchanger 204 in Figure 10), about 11.5 MW heat is transferred to the condenser of the heat pump. A compressor is needed to increase the ammonia pressure to 42 bar and the temperature to  $191^\circ\text{C}$ . The coefficient of performance (COP) of 3.2 is calculated and, 3.6 MW electrical power is required for the compressor. In the condenser, 15.0 MW heat is transferred to the struvite decomposition reactor. The pressure decreases to 5.5 bar in the expansion valve. The ammonia-rich flow from distillation tower is heated up again to  $90^\circ\text{C}$  with hot water from the bottom stream of the distillation tower (in heat exchanger #4). In Section 5.3, the influence of the ammonia concentration on the SOFC system will be investigated.

The main assumptions for the Cycle Tempo model are presented in Table 5. The outlet temperature of the wastewater (35°C) is considered to be high enough for a low-temperature thermal pre-treatment (mesophilic condition) of sludge for anaerobic digestion [7]. The circulation air with a temperature of 90°C is provided to heat the struvite (heat exchanger 402 in



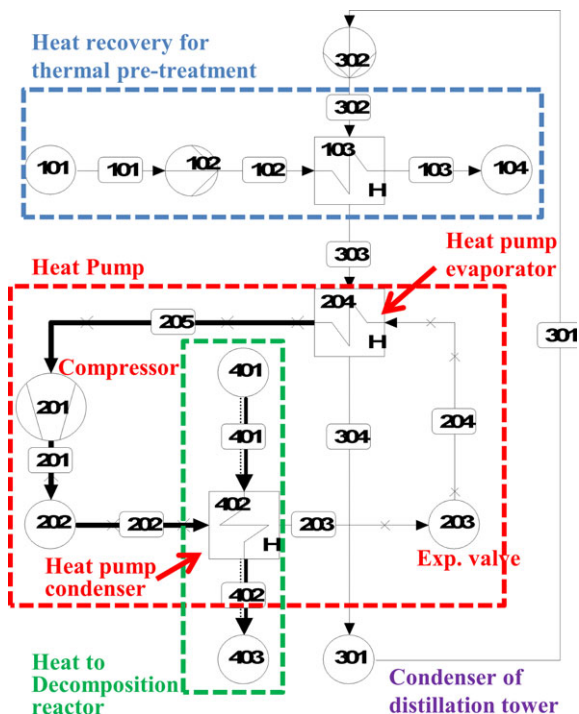


Fig. 10 Modeling of a heat pump assisted distillation tower with cooling cycle on Cycle-Tempo software.

Figure 10), and struvite heats up further with flue gas from the SOFC system. Produced ammonia is used in the same SOFC system with minor modifications. With a higher concentration of ammonia, a higher current density in the SOFC can be achieved.

### 4.3 SOFC Operating with High Ammonia Concentration

In the previous section, an ammonia recovery system with a heat pump assisted distillation tower has been explained. In this section, the influence of ammonia concentration on the performance of an ammonia-SOFC system is assessed. Various ammonia concentrations, along with specified fuel flow rates (see Table 4) have been used for the same ammonia-SOFC model developed for a fuel stream with an ammonia concentration of 14 mol.%. The amount of ammonia in the fuel streams ( $1.33 \text{ kg s}^{-1}$ ) has been kept constant for the model with different ammonia concentrations, and the fuel flow rates have been changed accordingly. Because of different flow rates and

Table 5 Assumptions of heat pump assisted distillation tower model.

Parameter		Value
Condenser of distillation tower:	Vapour outlet	50 °C
	Water outlet	40 °C
Heat Ex. #103 (Figure 10):	Circulation water outlet	30 °C
	Wastewater inlet temp.	15 °C
	Wastewater outlet temp.	35 °C
Compressor:	Isentropic efficiency	75%
	Mechanical efficiency	95%
Pumps:	Mechanical efficiency	80%
Pressure drop:	Heat exchanger	0.1 / bar

the temperature of fuel stream, the LHV of the fuel is slightly different, although the mass flow rate of pure ammonia is constant for different cases. The cell resistance is kept constant for different models. The cell voltage is calculated by the model accordingly. Minor modifications (such as overall fuel utilization and anode/cathode recirculation ratios) are required to optimize the system operation in terms of power generation, for different ammonia concentrations. Results of Cycle-Tempo modeling have been summarized in Table 6. Increasing the ammonia concentration from 14% to 30 mol.% increases energy and exergy efficiencies. The performance of the developed system shows an excellent potential to be used for aqueous ammonia (ammonium hydroxide liquid fuel) with roughly 28% ammonia by mass (30 mol.%). With further increasing the ammonia concentration, energy efficiency of the system relatively increases.

Since the concentration of ammonia is increased to 90%, the fuel flow rate decreases to  $1.49 \text{ kg s}^{-1}$ . The Nernst voltage for the highest ammonia concentration (90%) is 1.09 V, and higher current density and higher fuel utilization are achievable (Figure 5). This leads to increasing the SOFC power production (13.50 MW) at higher fuel utilization (89%), current density ( $2,150 \text{ A m}^{-2}$ ) and higher cell voltage (0.67 V) in comparison with a system operating on low ammonia concentration. Increasing the ammonia concentration to 90% increases the system efficiency by 4.6% in comparison to SOFC fuelled with aqueous ammonia with 14 mol.%. Moreover, the power density of the SOFC stack increases significantly by 48% (Table 6). This implies that the required cell area (the number of cells) decreases by increasing the ammonia concentration in the fuel.

Table 6 Ammonia-SOFC system results with different ammonia concentration in Cycle Tempo.

Fuel stream		Cell voltage / V	CD / $\text{A m}^{-2}$	Overall $\text{U}_f$ / %	Air-fuel ratio ( $\lambda$ )	Power density / $\text{kW m}^{-2}$	Energy generation		Net efficiency	
Ammonia / mol.%	Flow rate / $\text{kg s}^{-1}$						Power / MW	Heat / MW	Energy / %	Exergy / %
14	10.0	0.67	1,450	82	1.5	0.97	12.42	12.35	48.5	39.0
30	4.62	0.67	1,600	84	4.1	1.10	12.91	11.20	50.7	45.0
60	2.27	0.67	1,950	87	5.7	1.32	13.20	11.28	51.8	47.9
90	1.49	0.67	2,150	89	8.6	1.44	13.51	11.48	53.1	50.9

Per-pass fuel utilization still has been kept around 80%. On the other hand, low steam concentration in the fuel increases required air ( $14.9 \text{ kg s}^{-1}$ ) for cooling the SOFC stack, and this increases lambda in the afterburner ( $\lambda = 8.6$ ). The heat generated in the SOFC and afterburner can be partially transferred to the struvite decomposition reactor at a very high temperature ( $610^\circ\text{C}$ ). However, in comparison with the lower concentrations, less heat is delivered to the decomposition reactor (11.48 MW). The temperature of the flue gas stream to the environment is  $60^\circ\text{C}$ . This temperature is lower than the flue gas temperature for other cases because of the low concentration of water in the system, and this makes the system more efficient. The ammonia-SOFC system net energy efficiency is 53.1%.

Exergy destruction of the ammonia-SOFC system fed with a high concentration of ammonia (90 mol.%) is shown in Figure 11. Due to the lower fuel flow rate, the exergy input, in this case, is slightly lower (26.54 MW). Exergy destructions take place in all components, mostly in the fuel cell with 11.5%, and heat exchangers in the fuel/air preheating process with 8.3%. Exergy losses in the afterburner are 3.2%, which is attributed to the high fuel utilization in the SOFC fuelled with rich-ammonia gas. Only 2.1% of fuel exergy is transferred to the stack (exhaust), and this makes the system more efficient compared to system fuelled with lower ammonia concentrations since 14.6% of the fuel exergy is transferred to the decomposition reactor. The total exergy efficiency of this system, including the exergy of heat transferred to the struvite decomposition reactor, is 65.5%.

The achieved exergy efficiency of 50.9% in this system is comparable with the values presented in the literature for SOFC-GT system [21] with exergy efficiency of 55.1%. The difference is due to a lower ammonia concentration in the fuel (90 mol.%), lower operating temperature and higher cell resistance ( $1.0 \times 10^{-4} \Omega \text{ m}^2$ ).

## 4.4 Integrated System

Finally, the energy balance of the ammonia-SOFC system, integrated with a heat pump assisted distillation tower and precipitation process is investigated in this section. The SOFC supplies part of the struvite decomposition heat demand and the heat pump provides the rest. A heat pump is applied to extract heat from the condenser of the distillation tower. SOFC also provides electrical power for the compressor of the heat pump. Meanwhile, the heat required for thermal pre-treatment ( $35^\circ\text{C}$ ) of  $100 \text{ kg s}^{-1}$  of wastewater sludge is supplied (8.4 MW). This integration makes the system sustainable since there is still net electrical power generated by the SOFC ( $9.9 \text{ MW}_\text{E}$ ). The energy balance flow diagram of this system is illus-

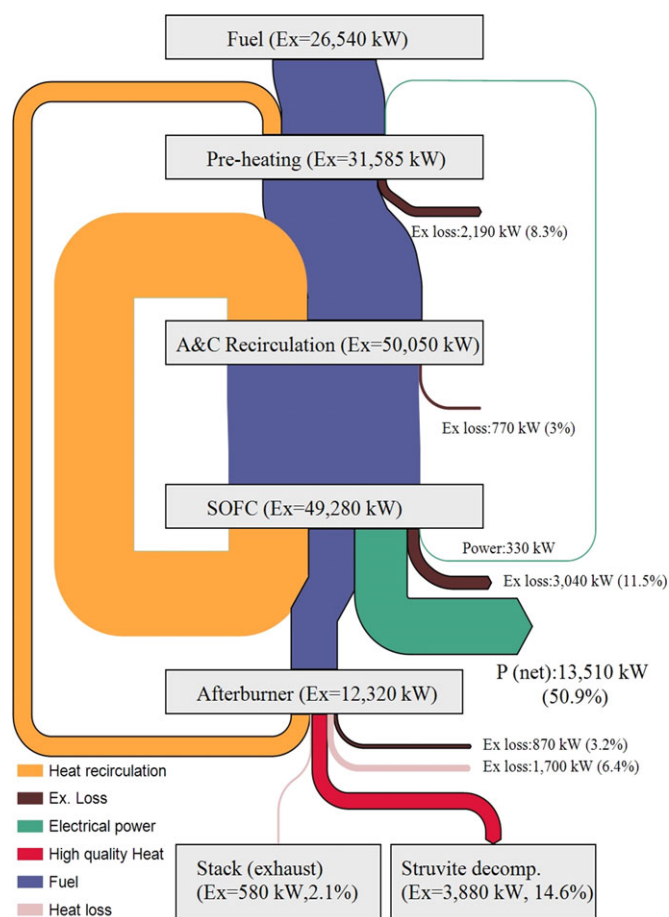


Fig. 11 Distribution of exergy losses in Ammonia-SOFC model with ammonia concentration of 90 mol.%.

trated in Figure 12. The net electrical efficiency of this system (including energy demand of the heat pump assisted distillation tower) is 39% based on ammonia LHV ( $18.6 \text{ MJ kg}^{-1}$ ) of the ammonia-water mixture.

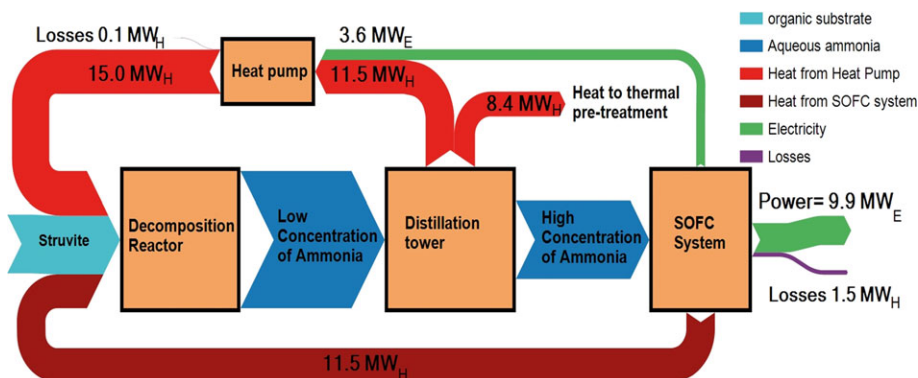


Fig. 12 Energy balance flow diagram of Ammonia-SOFC model and heat pump assisted distillation tower with ammonia concentration of 90 mol.%.

## 5 Conclusions

Nitrogen removal from wastewater treatment is known as an energy-intensive process. Struvite precipitation is one of the methods of nutrient (Phosphorus and nitrogen) removal in wastewater. Struvite can be decomposed to ammonia water mixture by heating at an optimum temperature of 106 °C. The concentration of produced aqueous ammonia in this process is very low (14.2 mol.%) but, can be used as fuel in an SOFC system. Feasibility of operating an SOFC with different concentration of ammonia is investigated by conducting experiments at 800 °C. Ammonia is fully cracked inside the SOFC at this operating temperature. Subsequently, a model incorporating a fuel cell with ammonia recovery (precipitation) process is developed. The energy and exergy efficiencies of this system were 48.5% and 39%, respectively. However, in this system, the required heat for struvite decomposition could not be generated by the SOFC system (stack and afterburner).

To make the system self-supporting and more efficient, the concentration of ammonia in the fuel stream is shown to be increased by integrating a distillation tower to the system. A heat pump is coupled with the distillation tower to satisfy the heat duty of the condenser of the distillation tower and reduce the temperature of the outlet stream. The higher concentration of ammonia improves the ammonia-SOFC system efficiency. The heat pump and SOFC system supply the heat required for the struvite decomposition reactor (see Figure 9). The net energy and exergy efficiencies of the ammonia-SOFC system operating with an aqueous solution of ammonia (90% ammonia mole fraction) are 53.1% and 49.6%, respectively. On the one hand, extra investments are required for the heat pump and distillation tower, on the other hand, less SOFC area (number of cells) is required for the SOFC stack and the overall electrical efficiency increases. The net energy efficiency of the integrated SOFC system with heat pump assisted distillation tower is around 39% (ammonia LHV-based). After assessment of the ammonia-SOFC system, the next step would be the evaluation of a SOFC system with an ammonia-biogas mixture as a fuel. Sustainability of conventional WWTP can be improved by applying SOFC as a heat and power generation device. However, techno-economic evaluation of the designed system should be carried out to develop this system from the laboratory to the industrial scale.

## Appendix

### Heat usage calculation

Based on the thermogravimetric analysis (TGA) measurements, it is possible to determine the heat required for the decomposition of struvite. The Q600 unit from TGA instruments measures the temperature rise due to the heating of the furnace of the sample and a reference. The temperature difference ( $\Delta T$ ) between the two is used to determine the net heat flow into or out of the sample during the experiment. While no transitions take place in the sample, the sample tempera-

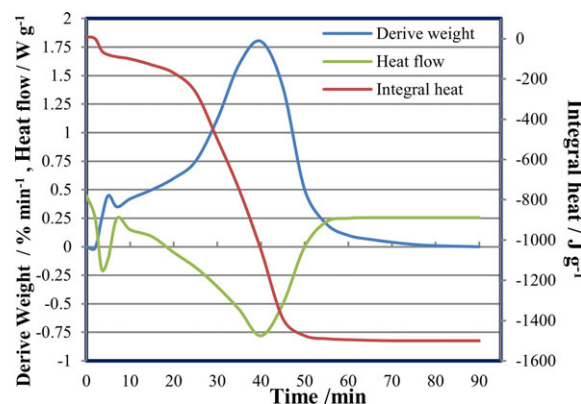


Fig. 13 Integrated heat flow for evaporating ammonia water mixture in struvite decomposition reactor.

ture will track the reference temperature. This  $\Delta T$  signal is then used to calculate the heat flow for the reaction. Endothermic reactions such as melting and evaporation will result in a negative heat flow curve, whereas exothermic reactions such as oxidation will result in a positive heat flow curve. Three distinct struvite samples (20–30 mg) with different free water concentrations have been tested. First, the oven is closed, and nitrogen is purged for around 20 min to provide an inert environment. The oven is heated up to 80 °C and kept at that temperature for about 20 min to release most of the free water. Then, TGA experiments are conducted in a range of from 80 °C to 160 °C with a ramp of 1 °C min<sup>-1</sup>. Results show that the struvite samples lose their water and ammonia simultaneously during decomposition. Most of the water and the ammonia is evaporated around 90 °C, and it is observed that weight loss is less significant after 110 °C. As an example, combined graphs for a struvite sample (with maximum water content) are shown in Figure 13 with the weight loss per minute, the heat flow and the integrated heat flow during the experiment.

Struvite samples (with different free water concentrations) demonstrate a negative heat flow, between 1,000 kJ kg<sup>-1</sup> to 1,500 kJ kg<sup>-1</sup>, in comparison to the reference. In this study, it is assumed that the heat required for struvite decomposition is 1,350 kJ kg<sup>-1</sup>. Based on decomposition reaction Eq. (2), 1 kg struvite decomposes into 510 g of ammonia water vapour and 490 g of MHP. Therefore, the heat required for producing ammonia-water mixture is 2,650 kJ kg<sup>-1</sup>. This is higher than the heat of vaporization of ammonia-water mixture with 14% ammonia (2,350 kJ kg<sup>-1</sup>). Moreover, it is seen that concentrations of struvite did not change due to heating, and there was no sulfur-containing compound in the vapour stream (which is hazardous for SOFC).

## Acknowledgements

The authors would like to thank Mr. Hans van Zalen and Sander Tensen for their efforts in conducting an experimental evaluation on the struvite decomposition in the Fuel Cell lab at Delft University of Technology.

## List of Symbols

### Nomenclature

AD	Anaerobic digestion
AGR	Anode gas recirculation
ASR	Area specific resistance
BOD	Biochemical oxygen demand
BoP	Balance of plant
CD	Current density
CEM	Controlled evaporation and mixing
CHP	Combined heat and power
CSTR	Continuous stirred tank reactor
DIR	Direct internal reforming
DO	Dissolved oxygen
DTGA	Derivative thermogravimetric analysis
E	Voltage / V
EIS	Electronic impedance spectroscopy
ESC	Electrolyte supported cell
Ex.	Expansion
GC	Gas chromatography
GDC	Gadolinium doped ceria
GHG	Greenhouse gas
h	Hours
IC	Internal combustion
LHV	Lower heating value / kJ mol <sup>-1</sup>
MAP	Magnesium ammonium phosphate
MFC	Mass flow meter
MHP	Magnesium hydrogen phosphate
ms	Milliseconds
N	Nitrogen
OCV	Open circuit voltage
P	Partial pressure
PO	Phosphorus
ppm	part per million
R	Universal gas constant
SOFC	Solid oxide fuel cell
T	Absolute temperature / K
TAN	Total ammonia nitrogen
TN	Total nitrogen
TGA	Thermogravimetric analysis
UASB	Up-flow anaerobic sludge blanket
U <sub>f</sub>	Fuel utilization factor
V	Potential / V
W	Mechanical work
WWT	Wastewater treatment plant
YSZ	Yttria-stabilized zirconia

### Greek letters

$\Delta H^0$	Enthalpy change / kJ mol <sup>-1</sup>
$\lambda$	Air factor
$\Omega$	Ohmic resistance

## References

- [1] W. Mo, Q. Zhang, *J. Environ. Manage.* **2013**, 127, 255.
- [2] S. E. Hosseini, M. A. Wahid, *Renewable and Sustainable Energy Reviews* **2013**, 19, 454.
- [3] M. Mosayeb-Nezhad, A. S. Mehr, M. Gandiglio, A. Lanzini, M. Santarelli, *Applied Thermal Engineering* **2018**, 129, 1263.
- [4] W. Verstraete, P. V. de Caveye, V. Diamantis, *Bioresource Technology* **2009**, 100, 5537.
- [5] B. Wett, K. Buchauer, C. Fimml, *IWA Leading Edge Technology Conference*, **2007**, pp. 21–24.
- [6] S. Sengupta, T. Nawaz, J. Beaudry, *Current Pollution Reports* **2015**, 1, 155.
- [7] S. A. Saadabadi, A. Thallam Thattai, L. Fan, R. E. F. Lindeboom, H. Spanjers, P. V. Aravind, *Renewable Energy* **2019**, 134, 194.
- [8] E. Grönlund, **2014**.
- [9] P. D. Jenssen, L. Vråle, O. Lindholm, *Proceedings of International Conference on Natural Resources and Environmental Management and Environmental Safety and Health*, Kuching, Malaysia, **2007**, 2729.
- [10] G. A. Burton Jr., R. Pitt, *Stormwater Effects Handbook: A Toolbox for Watershed Managers, Scientists, and Engineers*, CRC Press, Boca Raton, FL, USA, **2001**.
- [11] P. Habermeyer, A. Sánchez, *Water Environment. Research* **2005**, 77, 229.
- [12] J. Serralta, J. Ribes, A. Seco, J. Ferrer, *Water Science and Technology* **2002**, 45, 309.
- [13] G. D. Zupančič, M. Roš, *Bioresource Technology* **2008**, 99, 100.
- [14] D. J. Kinnear, M.-L. Pellegrin, T. B. Cross, M. J. Condran, T. Kochaba, C. M. Haney, *Proceedings of the Water Environment Federation* **2010**, 2010, 18.
- [15] K. Hemmes, P. Luimes, A. Giesen, A. Hammenga, P. Aravind, H. Spanjers, *Water Practice and Technology* **2011**, 6, wpt20110071.
- [16] N. Morales, M. A. Boehler, S. Buettner, C. Liebi, H. Siegrist, *Water* **2013**, 5, 1262.
- [17] C. Zamfirescu, I. Dincer, *Journal of Power Sources* **2008**, 185, 459.
- [18] J. Larminie, A. Dicks, M. S. McDonald, *Fuel Cell Systems Explained*, Vol. 2, Wiley, New York, NY, USA, **2003**.
- [19] A. Afif, N. Radenahmad, Q. Cheok, S. Shams, J. H. Kim, A. K. Azad, *Renewable and Sustainable Energy Reviews* **2016**, 60, 822.
- [20] A. Fuerte, R. X. Valenzuela, M. J. Escudero, L. Daza, *Journal of Power Sources* **2009**, 192, 170.
- [21] H. C. Patel, T. Woudstra, P. V. Aravind, *Fuel Cells* **2012**, 12, 1115.
- [22] N. Cherkasov, A. O. Ibadon, P. Fitzpatrick, *Chemical Engineering and Processing: Process Intensification* **2015**, 90, 24.
- [23] R. Michalsky, A. Avram, B. Peterson, P. H. Pfromm, A. Peterson, *Chemical Science* **2015**, 6, 3965.

- [24] D. Frattini, G. Cinti, G. Bidini, U. Desideri, R. Cioffi, E. Jannelli, *Renewable Energy* **2016**, 99, 472.
- [25] L. F. Razon, *Environmental Progress and Sustainable Energy* **2014**, 33, 618.
- [26] W. T. Mook, M. H. Chakrabarti, M. K. Aroua, G. M. A. Khan, B. S. Ali, M. S. Islam, M. A. Abu Hassan, *Desalination* **2012**, 285, 1.
- [27] R. Y. Surampalli, S. K. Banerji, J. Chen, *Journal of Environmental Engineering* **1993**, 119, 493.
- [28] Y. Liu, *Wastewater Purification: Aerobic Granulation in Sequencing Batch Reactors*, CRC Press, Boca Raton, FL, USA, **2007**.
- [29] V. Larsson, **2011**.
- [30] M. Maurer, P. Schwegler, T. Larsen, *Water Science and Technology* **2003**, 48, 37.
- [31] T. A. Larsen, W. Gujer, *Water Science and Technology* **1996**, 34, 87.
- [32] M. Strous, J. J. Heijnen, J. G. Kuenen, M. S. M. Jetten, *Appl. Microbiol. Biotechnol.* **1998**, 50, 589.
- [33] I. Martin, M. Pidou, A. Soares, S. Judd, B. Jefferson, *Environmental Technology* **2011**, 32, 921.
- [34] Y. Chen, J. J. Cheng, K. S. Creamer, *Bioresource Technology* **2008**, 99, 4044.
- [35] K. H. Hansen, I. Angelidaki, B. K. Ahring, *Water research* **1998**, 32, 5.
- [36] O. Yenigün, B. Demirel, *Process Biochemistry* **2013**, 48, 901.
- [37] A. Serna-Maza, S. Heaven, C. J. Banks, *Bioresource Technology* **2014**, 152, 307.
- [38] L. Zhang, Y.-W. Lee, D. Jahng, *Journal of Hazardous Materials* **2012**, 199, 36.
- [39] S. Montalvo, L. Guerrero, R. Borja, E. Sánchez, Z. Milán, I. Cortés, M. Angeles de la la Rubia, *Applied Clay Science* **2012**, 58, 125.
- [40] L. Xu, F. Dong, H. Zhuang, W. He, M. Ni, S.-P. Feng, P.-H. Lee, *Energy Conversion and Management* **2017**, 140, 157.
- [41] L. Lin, S. Yuan, J. Chen, Z. Xu, X. Lu, *Journal of Hazardous Materials* **2009**, 161, 1063.
- [42] M. Mondor, L. Masse, D. Ippersiel, F. Lamarche, D. Masse, *Bioresource technology* **2008**, 99, 7363.
- [43] V. K. Gupta, H. Sadegh, M. Yari, R. Shahryari Ghoshe-kandi, B. Maazinejad, M. Chahardori, *Global Journal of Environmental Science and Management* **2015**, 1, 149.
- [44] X. Wang, X. Zhang, Y. Wang, Y. Du, H. Feng, T. Xu, *Journal of Membrane Science* **2015**, 490, 65.
- [45] A. K. Luther, J. Desloover, D. E. Fennell, K. Rabaey, *Water Research* **2015**, 87, 367.
- [46] W. Verstraete, P. Van de Caveye, V. Diamantis, *Bio-resource Technology* **2009**, 100, 5537.
- [47] A. Mulder, *Water Science and Technology* **2003**, 48, 67.
- [48] Y.-Q. Chen, J.-J. Tang, W.-L. Li, Z.-H. Zhong, J. Yin, *Transactions of Nonferrous Metals Society of China* **2015**, 25, 497.
- [49] A. Gunay, D. Karadag, I. Tosun, M. Ozturk, *Journal of Hazardous Materials* **2008**, 156, 619.
- [50] C. K. Chauhan, M. J. Joshi, *Journal of Crystal Growth* **2013**, 362, 330.
- [51] A. Sarkar, *Journal of Materials Science* **1991**, 26, 2514.
- [52] J. Staniforth, R. M. Ormerod, *Ionics* **2003**, 9, 336.
- [53] M. Ni, M. K. Leung, D. Y. Leung, *International Journal of Energy Research* **2009**, 33, 943.
- [54] A. Chellappa, C. Fischer, W. Thomson, *Applied Catalysis A: General* **2002**, 227, 231.
- [55] G. G. M. Fournier, I. W. Cumming, K. Hellgardt, *Journal of Power Sources* **2006**, 162, 198.
- [56] G. Cinti, U. Desideri, D. Penchini, G. Discepoli, *Fuel Cells* **2014**, 14, 221.
- [57] N. J. J. Dekker, G. Rietveld, *Journal of Fuel Cell Science and Technology* **2006**, 3, 499.
- [58] R. Lan, S. Tao, *Frontiers in Energy Research* **2014**, 2, 35.
- [59] L. Zhang, W. Yang, *Journal of Power Sources* **2008**, 179, 92.
- [60] K. Xie, Q. Ma, B. Lin, Y. Jiang, J. Gao, X. Liu, G. Meng, *Journal of Power Sources* **2007**, 170, 38.
- [61] G. Y. Meng, C. R. Jiang, J. J. Ma, Q. L. Ma, X. Q. Liu, *Journal of Power Sources* **2007**, 173, 189.
- [62] L. M. Liu, K. N. Sun, X. Y. Wu, X. K. Li, M. Zhang, N. Q. Zhang, X. L. Zhou, *Int. J. Hydrogen. Energ.* **2012**, 37, 10857–10865.
- [63] M. Ni, M. K. H. Leung, D. Y. C. Leung, *International Journal of Energy Research* **2009**, 33, 943.
- [64] Q. Ma, R. Peng, Y. Lin, J. Gao, G. Meng, *Journal of Power Sources* **2006**, 161, 95.
- [65] Q. Ma, R. Peng, L. Tian, G. Meng, *Electrochemistry Communications* **2006**, 8, 1791.
- [66] S. Farhad, F. Hamdullahpur, *Journal of Power Sources* **2010**, 195, 3084.
- [67] M. Rokni, *Energy* **2013**, 61, 87.
- [68] E. Baniasadi, I. Dincer, *Int. J. Hydrogen. Energ.* **2011**, 36, 11128.
- [69] F. Leucht, W. G. Bessler, J. Kallo, K. A. Friedrich, H. Müller-Steinhagen, *Journal of Power Sources* **2011**, 196, 1205–1215.
- [70] S. Chan, H. Ho, Y. Tian, *Int. J. Hydrogen Energ.* **2003**, 28, 889.
- [71] N. Dekker, G. Rietveld, *Journal of fuel cell science and technology* **2006**, 3, 499.
- [72] Cycle-Tempo Documentation, can be found under [www.asimptote.nl/software/cycle-tempo/cycle-tempo-documentation/](http://www.asimptote.nl/software/cycle-tempo/cycle-tempo-documentation/), (accessed 12 December 2019).
- [73] J. D. Seader, E. J. Henley, D. K. Roper, **1998**.
- [74] B. Metcalf Eddy, *Wastewater Engineering: Treatment Disposal Reuse*, McGraw-Hill, New York, USA, **1980**.
- [75] M. K. Ghose, *Water Research* **2002**, 36, 1127.
- [76] A. K. Jana, *Energy Conversion and Management* **2014**, 77, 287.
- [77] H. Li, N. Russell, V. Sharifi, J. Swithenbank, *Desalination* **2011**, 281, 118.